

Development of the method for identification of the unknown short duration source in urban atmospheric environment using the CFD model

Ivan V. Kovalets^a, George C. Efthimiou^b, Alexandros Venetsanos^b, Spyros Andronopoulos^b, Christos D. Argyropoulos^c, Konstantinos Kakosimos^c

^aDepartment of Environmental Modelling, Institute of Mathematical Machine and System Problems, National Academy of Sciences of Ukraine, Kiev, Ukraine

^bEnvironmental Research Laboratory, INRASTES, NCSR Demokritos, Patriarchou Grigoriou & Neapoleos Str., 15310, Aghia Paraskevi, Greece

^cDepartment of Chemical Engineering & Mary Kay 'O Connor Processes Safety Center, Texas A&M University at Qatar, Education City, Doha, Qatar, PO Box 23874

Introduction (I)

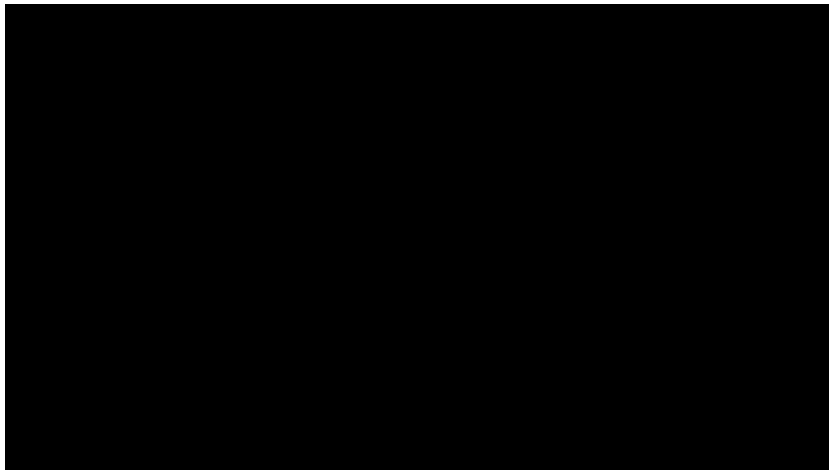
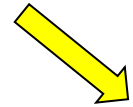
- The characterization of an unknown atmospheric pollutant's source following a release is a special case of inverse atmospheric dispersion problem.
- Such kind of inverse problems are to be solved in a variety of application areas such as:
 - **emergency response**
 - **pollution control decisions**
 - **indoor air quality**
 - **monitor of nuclear testing**

Introduction (II)

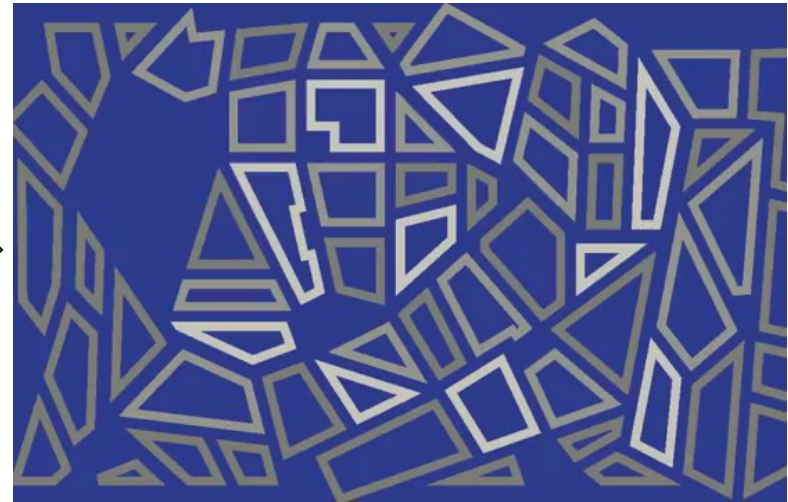
Release of a hazardous airborne material from a point source upwind or inside an urban area.

wind

Continuous release



wind



EWTL, University of Hamburg.

LES simulations by V. Fuka with
CLMM code, Charles University
(Prague).

Continuous release - Inverse problem

Prediction of

- 1) The location of the source,
- 2) The source emission rate.

State of the art (I)

- In the urban or industrial plant spatial scale, there are few researchers that have combined **Computational Fluid Dynamics (CFD)** with **source estimation techniques**.

| | Publication | CFD code | Source estimation technique |
|-----|-----------------------|-----------------|------------------------------------|
| 1. | Keats et al., 2007 | urbanSTREAM | Probabilistic |
| 2. | Chow et al., 2008 | FEM3MP | Probabilistic |
| 3. | Bady et al., 2009 | Star-CD | Optimization |
| 4. | Kovalets et al., 2011 | ADREA-HF | Optimization |
| 5. | Libre et al., 2012 | Fluidyn-PANEPR | Probabilistic |
| 6. | Kumar et al., 2015 | fluidyn-PANACHE | Optimization |
| 7. | Kumar et al., 2016 | fluidyn-PANACHE | Optimization |
| 8. | Xue et al., 2017a | | |
| 9. | Xue et al., 2017b | | |
| 10. | Mons et al., 2017 | | |

State of the art (II)

- In the urban or industrial plant spatial scale, there are few researchers that have combined **Computational Fluid Dynamics (CFD)** with **source estimation techniques**.

| | Publication | CFD code | Source estimation technique |
|-----|------------------------------|-----------------|------------------------------------|
| 1. | Keats et al., 2007 | urbanSTREAM | Probabilistic |
| 2. | Chow et al., 2008 | FEM3MP | Probabilistic |
| 3. | Bady et al., 2009 | Star-CD | Optimization |
| 4. | <u>Kovalets et al., 2011</u> | <u>ADREA-HF</u> | <u>Optimization</u> |
| 5. | Libre et al., 2012 | Fluidyn-PANEPR | Probabilistic |
| 6. | Kumar et al., 2015 | fluidyn-PANACHE | Optimization |
| 7. | Kumar et al., 2016 | fluidyn-PANACHE | Optimization |
| 8. | Xue et al., 2017a | | |
| 9. | Xue et al., 2017b | | |
| 10. | Mons et al., 2017 | | |

State of the art (III)

- In the urban or industrial plant spatial scale, there are few researchers that have combined **Computational Fluid Dynamics (CFD)** with **source estimation techniques**.

| | Publication | CFD code | Source estimation technique |
|-----|------------------------|-----------------|------------------------------------|
| 1. | Keats et al., 2007 | urbanSTREAM | Probabilistic |
| 2. | Chow et al., 2008 | FEM3MP | Probabilistic |
| 3. | Bady et al., 2009 | Star-CD | Optimization |
| 4. | Kovalets et al., 2011 | ADREA-HF | Optimization |
| 5. | Libre et al., 2012 | Fluidyn-PANEPR | Probabilistic |
| 6. | Kumar et al., 2015 | fluidyn-PANACHE | Optimization |
| 7. | Kumar et al., 2016 | fluidyn-PANACHE | Optimization |
| 8. | Xue et al., 2017a | | |
| 9. | Xue et al., 2017b | | |
| 10. | Mons et al., 2017 | | |
| 11. | Efthimiou et al., 2017 | ADREA-HF | Optimization |

Efthimiou et al., 2017

Atmospheric Environment, 170, 118-129.

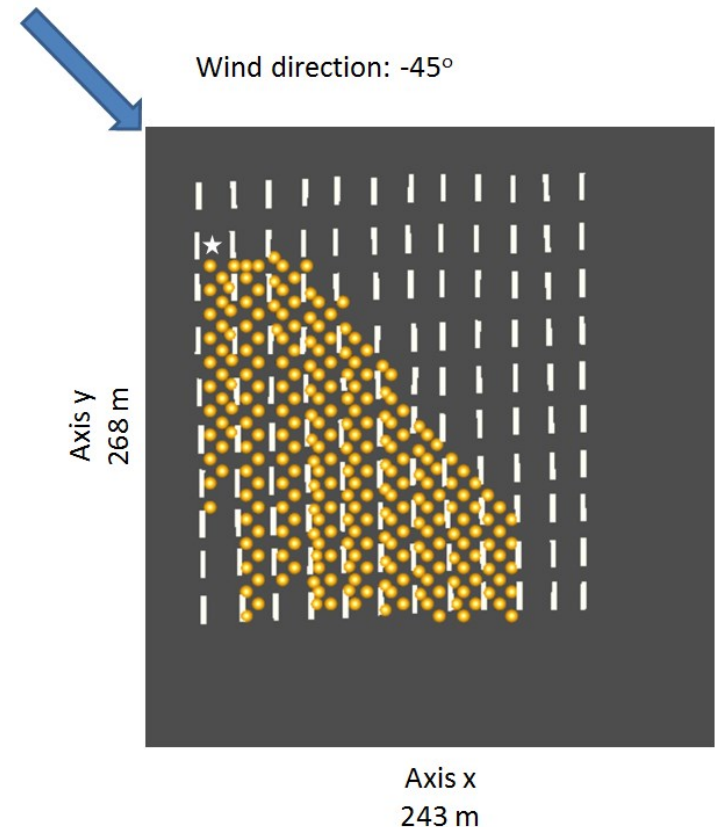
Results of the Coarse grid

| Method | r_H (m) | r_V (m) | δq (-) |
|--|-----------|-----------|----------------|
| New | 2.99 | 0.1 | 1.42 |
| Old (no prior information) | 2.99 | 0.1 | 1.42 |
| Old (prior information, $\sigma_M=10^{-9}$) | 2.99 | 0.1 | 1.42 |
| Old (prior information, $\sigma_M=10^{-8}$) | 2.99 | 0.1 | 1.42 |
| Old (prior information, $\sigma_M=10^{-7}$) | 5.44 | 0.1 | 1.06 |
| Old (prior information, $\sigma_M=10^{-6}$) | 18.48 | 0.1 | 1.11 |
| Old (prior information, $\sigma_M=10^{-5}$) | 18.48 | 0.1 | 1.11 |

Results of the Fine grid

| Method | r_H (m) | r_V (m) | δq (-) |
|--|-----------|-----------|------------------------|
| New | 1.20 | 0.1 | 1.69 |
| Old (no prior information) | 235.06 | 14.65 | 1.83×10^{-16} |
| Old (prior information, $\sigma_M=10^{-9}$) | 235.06 | 14.65 | 1.83×10^{-16} |
| Old (prior information, $\sigma_M=10^{-8}$) | 0.20 | 0.1 | 1.62 |
| Old (prior information, $\sigma_M=10^{-7}$) | 2.99 | 0.1 | 1.50 |
| Old (prior information, $\sigma_M=10^{-6}$) | 17.58 | 0.1 | 1.15 |
| Old (prior information, $\sigma_M=10^{-5}$) | 17.27 | 0.1 | 1.18 |

The validation was performed by simulating the MUST wind tunnel experiment.



Many releases of short duration (puffs) - Inverse problem

Prediction of

- 1) The location of the source,
- 2) The start time,
- 3) The release duration,
- 4) The inventory.

State of the art

- In the urban or industrial plant spatial scale, there are few researchers that have combined **Computational Fluid Dynamics (CFD)** with **source estimation techniques in transient case**

| Publication | CFD code | Source estimation technique |
|---------------------------|-----------------|------------------------------------|
| 1. Vervecken et al., 2015 | | |
| 2. Kovalets et al., 2017 | ADREA-HF | Optimization |

The goal of the present research

- Development of a source inversion algorithm and its integration in CFD Atmospheric Dispersion Modelling, allowing the assessment of the unknown source parameters for short duration releases in urban environment, assuming stationary meteorological conditions.

Source inversion algorithm

- Cost function – correlation taken with the negative sign

$$J = - \frac{\langle (c^o - \langle c^o \rangle)(c^c - \langle c^c \rangle) \rangle}{\sqrt{\langle (c^c - \langle c^c \rangle)^2 \rangle} \sqrt{\langle (c^o - \langle c^o \rangle)^2 \rangle}} \xrightarrow{\psi} \min$$

- Triangle brackets denote arithmetic averaging.
- ^o indicates observation.
- ^c indicates model.
- c indicates concentration.
- Minimized with respect to source location (x^s, y^s, z^s), time start of the release t^s and release duration Δ^s .
- Solution **does not** depend on source rate

Direct minimization algorithm

- Set of possible release locations coincide with the nodes of the computational grid

- Set of possible release durations is:

$$\Delta s: \{\Delta s_{\min}, 2 \cdot \Delta s_{\min}, \dots, N\delta \cdot \Delta s_{\min}\}$$

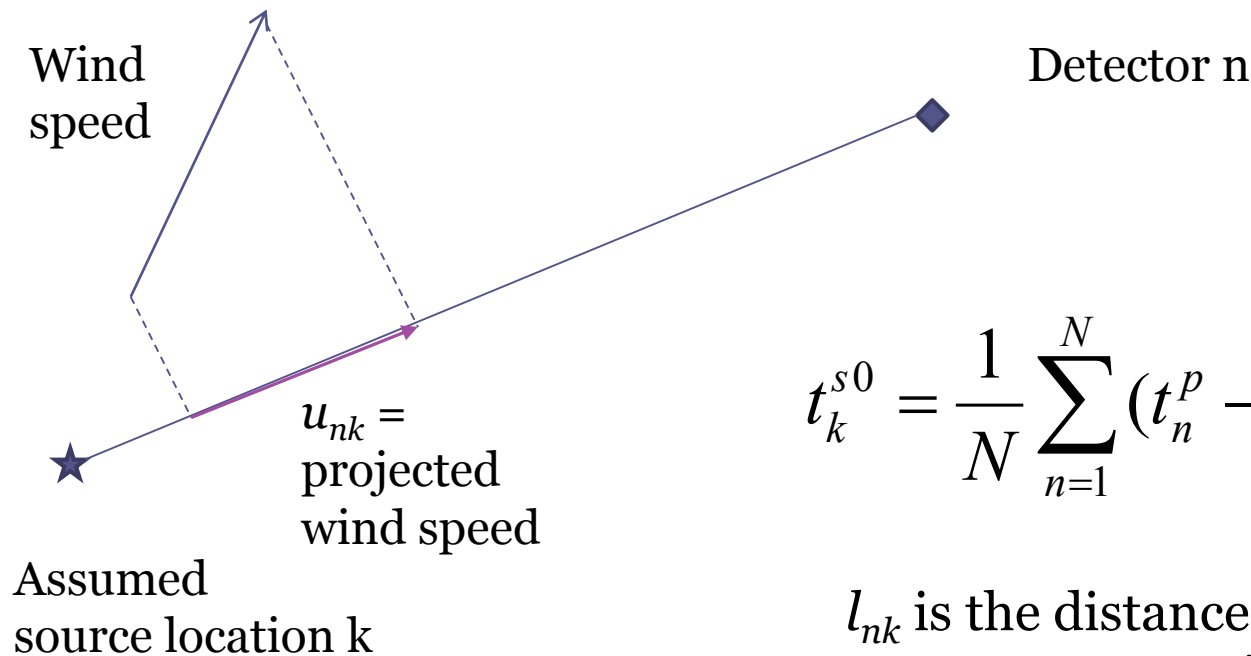
Δs_{\min} – is minimum release duration

Set of possible start times:

$$t_s: \{t_{s0}, t_{s0} \pm \Delta s, t_{s0} \pm 2\Delta s, \dots, t_{s0} \pm N\delta \cdot \Delta s\}$$

First guess approximation of the start time is evaluated for each assumed source location from:

- plume arrival time at a given sensor
- distance from sensor to assumed source location
- projected wind of the velocity



$$t_k^{s0} = \frac{1}{N} \sum_{n=1}^N (t_n^p - l_{nk} / u_{nk}),$$

l_{nk} is the distance between measurement point n and grid node k
Averaging by all sensors

Solution at sensor n , measurement time m for given set of assumed source parameters is expressed in the following SRF form:

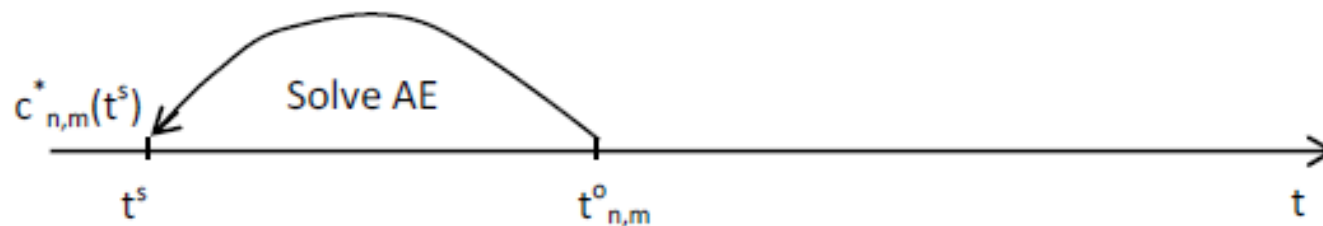
$$c_{n,m}^c = q^s \cdot \int_{t^s}^{t^s + \Delta^s} c_n^* \left(x^s, y^s, z^s, T - (t_{n,m} - t) \right) dt$$

c_n^* is adjoint variable. The r.h.s is the SRF. q^s is the source rate.

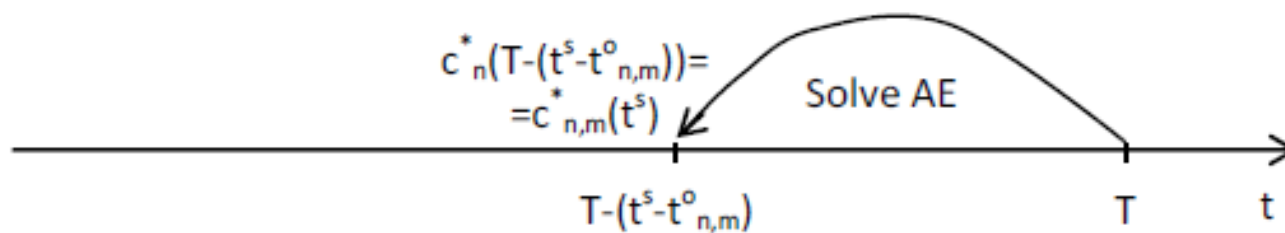
Source receptor function (SRF) is calculated by solving backward adjoint equations (AE)

Instead of solving AE for each measurement position and time, assuming stationary meteorology, AE is solved only once per measurement position with the non-zero impulse at $t=T$

Conventional scheme



Modified scheme



Computational issue

Number of Source Receptor Functions (SRF)

=

Number of the measurements of the time series!

=

Computationally prohibitive

Solution to computational issue

Integration of as many backward adjoint equations as the available measurement stations.

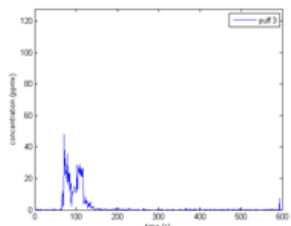
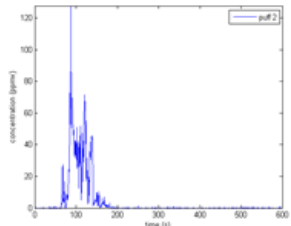
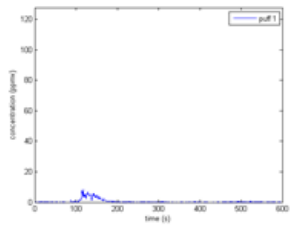


High numerical efficiency of the method.

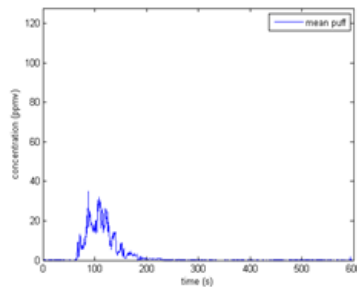
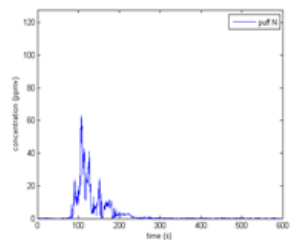
Consideration

The atmospheric dispersion problems characterized by small enough time intervals (<1 hour) and spatial scales up to 10 km from the release location for which the assumption of stationary meteorological fields is frequently applied in practice.

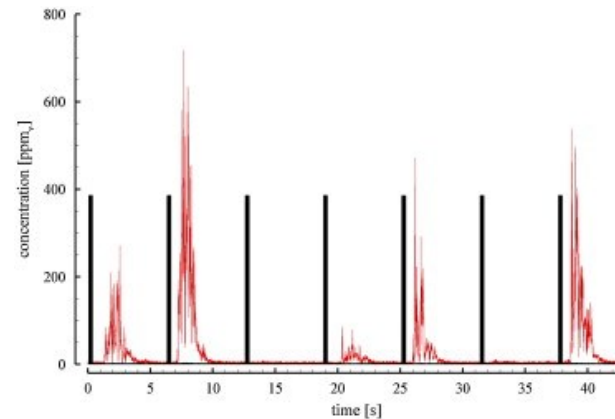
Setup of testing the method as two problems



...



- 1) Using ensemble averaged concentrations,
- 2) Using observations from individual puffs.



Note:

SRF was all the time the same since RANS model could not predict individual realizations, only their statistical properties.

The CUTE experiment (I)

<http://www.elizas.eu/>

The Complex Urban Test Experiment (CUTE) was carried out to test atmospheric dispersion models to be used for emergency response in case of accidental air pollution in urban areas.

Building heights between 25 and 35 m.



3725 m

3375 m

Geometry of the buildings in the area of the CUTE experiment and locations of sensors used in source inversion; source location is denoted by star; '+' – positions of real sensors; '◇' – positions of artificial sensors reporting zero values.

Harmo 18, Bologna,
October 2017

The CUTE experiment (II)

<http://www.elizas.eu/>

The concentration time series were measured by 16 sensors with about 1 s time resolution.

The experiment was repeated more than 200 times since the measurement signal was highly fluctuating due to turbulence. Thus each run of the same experiment (which we also call ‘ensemble member’) contains individual time histories of concentrations measured by each of the sensors



3725 m

3375 m

Geometry of the buildings in the area of the CUTE experiment and locations of sensors used in source inversion; source location is denoted by star; ‘+’ – positions of real sensors; ‘◊’ – positions of artificial sensors reporting zero values.

The wind field computational simulation (I)

| Domain dimensions x/y/z (m) | Grid characterization | Total number of cells | Number of cells in each axis | | |
|--------------------------------|-----------------------|-----------------------|------------------------------|-----|----|
| | | | x | y | z |
| 3725.2/3375.02/648 | “Coarse” | 61,488 | 72 | 61 | 14 |
| | “Fine” | 506,325 | 157 | 129 | 25 |

| Plane | Boundary condition |
|----------------|---|
| -x | Inlet: from separate 1D simulation vertical profiles for $u, v, k, \varepsilon, w=0$ |
| +x | Outlet: $\partial\varphi/\partial x = 0$, $\varphi=u, v, w, k, \varepsilon$ |
| -y | Inlet: from separate 1D simulation vertical profiles for $u, v, k, \varepsilon, w=0$ |
| +y | Outlet: $\partial\varphi/\partial y = 0$, $\varphi=u, v, w, k, \varepsilon$ |
| -z | Standard wall functions, roughness length = 1×10^{-5} m |
| +z | Fixed values for u, v, k, ε, w from cell mass balance (constant pressure) |
| Building walls | Standard wall functions, roughness length = 1×10^{-5} m |

The wind field computational simulation (II)

- For turbulence modelling, the standard $k-\varepsilon$ model was used.
- The unsteady Reynolds-Averaged Navier-Stokes equations for total mass, the 3 components of momentum, the turbulent kinetic energy and its dissipation rate were solved. The problem was treated as a transient case with a total simulation period of 1000 s.
- For the discretization of the convective terms in the momentum equations the upwind scheme was used.

The inverse source term estimation computations

| Plane | Boundary condition |
|-----------------------|--|
| -X | $\partial c^*/\partial x = 0$ |
| +X | $\partial c^*/\partial x = 0$ |
| -y | $\partial c^*/\partial y = 0$ |
| +y | $\partial c^*/\partial y = 0$ |
| -Z | $\partial c^*/\partial z = 0$ |
| +Z | $\partial c^*/\partial z = 0$ |
| Building walls | $\partial c^*/\partial s = 0, \mathbf{s}=\mathbf{x}, \mathbf{y}, \mathbf{z}$ |

- The total calculation time was set equal to the one used for the hydrodynamic computations, i.e., 1000s.
- For the discretization of the convective term in the adjoint equation the upwind scheme was used.
- The time step was kept constant and equal to 1s.

Results of calculations using ensemble averaged concentrations (I)

| Case | Obs. | Coarse grid- 16 sensors | Fine grid- 16 sensors | Coarse grid- 19 sensors | Fine grid- 19 sensors |
|---------------|--------|----------------------------|--------------------------|----------------------------|--------------------------|
| x^s, m | 228.72 | -16.5 | 156.53 | 195.55 | 181.57 |
| y^s, m | 294.64 | 192.62 | 294.36 | 251.90 | 319.42 |
| r_h, m | 0 | 265.6 | 72.2 | 54.1 | 53.3 |
| z^s, m | 0 | 13.5 | 6. | 13.5 | 18 |
| q^s, kg | 50 | 219 | 117.6 | 97.5 | 116.1 |
| t^s, s | 60 | 15.7 | 64.26 | 85.6 | 73.4 |
| Δ^s, s | 30 | 50 | 10 | 60 | 40 |
| Cor. coef. | 1 | 0.85 | 0.94 | 0.83 | 0.93 |

Results of calculations using ensemble averaged concentrations (II)

Environ Monit Assess (2017) 181:21–38
 October 2017

Projection on XY plane of the spatial distribution of the maximum correlation coefficient achieved in source inversion process depending on the location of the assumed source;

a),c) - results obtained on the coarse grid;

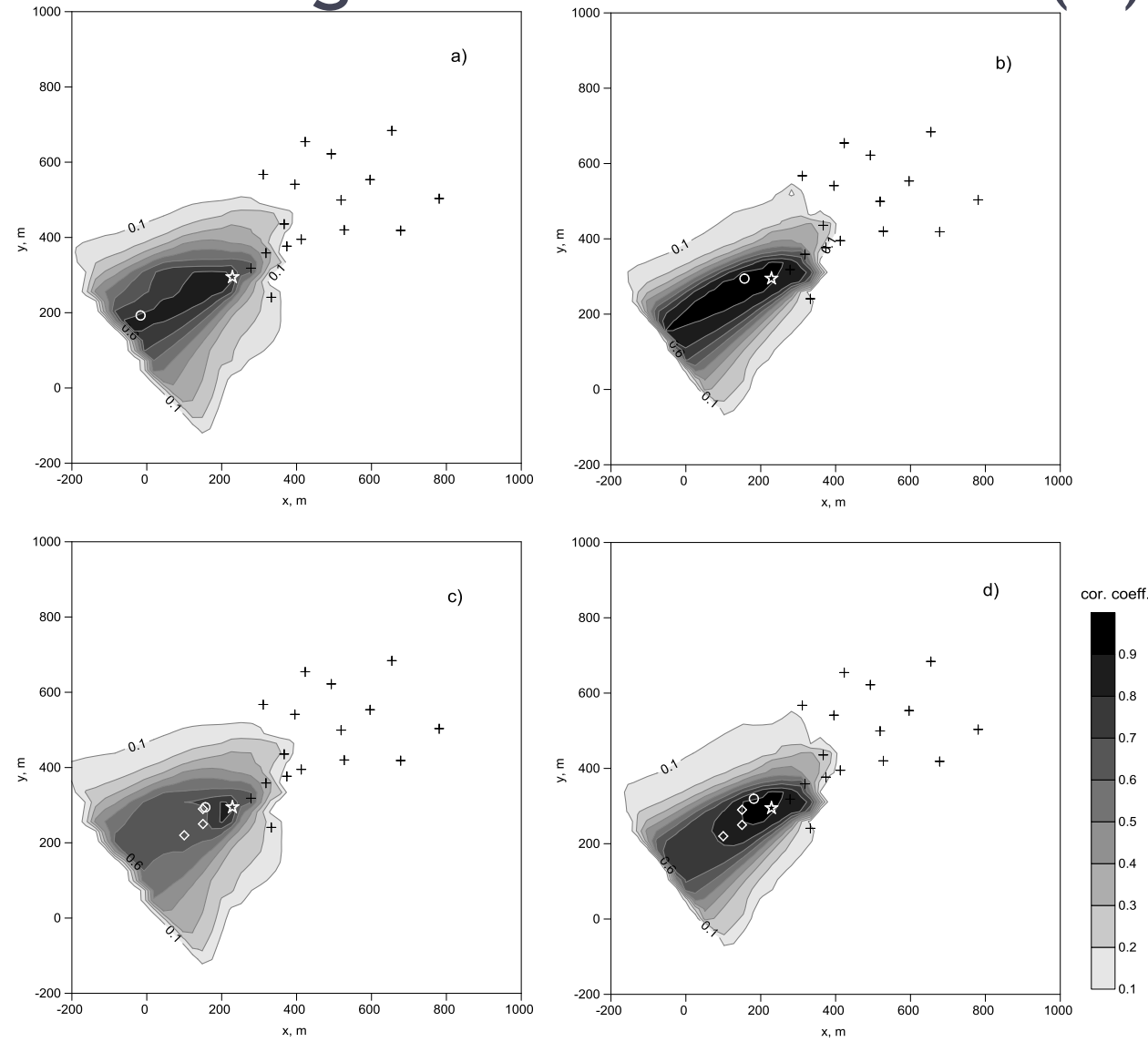
b),d) - results on fine grid;

upper – results obtained with using real data of 16 sensors;

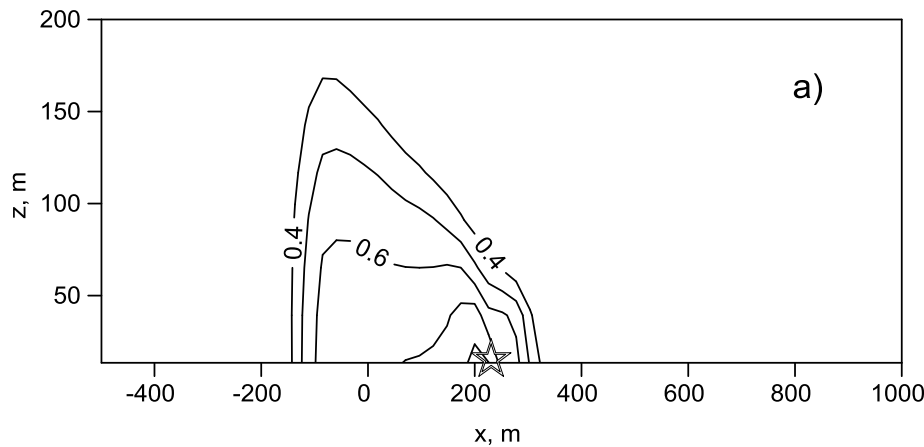
bottom - results obtained with using 3 additional artificial sensors reporting zero values;

white circle – estimated source location;

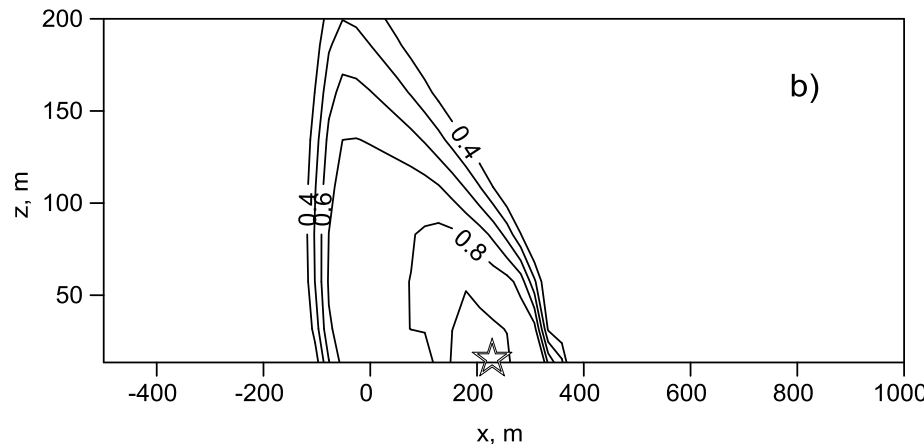
Isolines of the corr. coef. are drawn with the interval =0.1.



Results of calculations using ensemble averaged concentrations (III)



Projection on XZ plane of the spatial distribution of the maximum correlation coefficient of model results as compared to ensemble averaged measurements, achieved in source inversion process depending on the location of the assumed source;



a) - results obtained on coarse grid;

b) - results on fine grid.

Distributions only in the bottom part of the domain are shown; isolines of the corr. coef. are drawn with the interval =0.1;

star symbol denotes location of the source.

Computational times

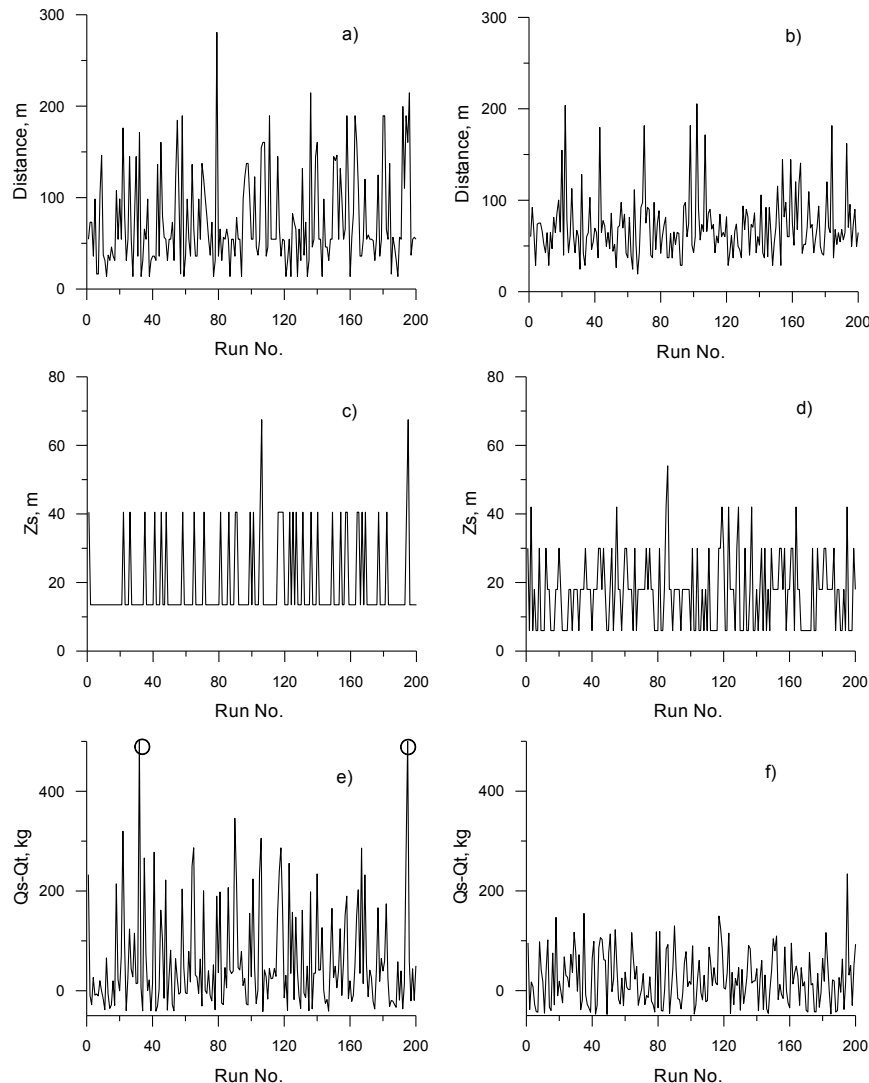
| Case | Number of active cells | Time of SRF calculation, h | Time of SRF calculation /1 sensor, h | Average time of single minimization run, h |
|--------|------------------------|----------------------------|--------------------------------------|--|
| Coarse | 61484 | 0.53 | 0.028 | 0.4 |
| Fine | 504966 | 2.82 | 0.148 | 2.8 |

The calculations were performed on personal computer with Intel® Core(TM) i5-4460 processor (4 cores), [CPU@3.2GHz](#) 16GB RAM.

The solution of backward adjoint equations during calculation of SRF was performed in parallel mode, but calculations of SRF for each of the sensors were performed sequentially.

Appropriate for real-time applications, especially taking in mind that much more powerful computers could be used.

Results of calculations using observations from individual puffs (I)

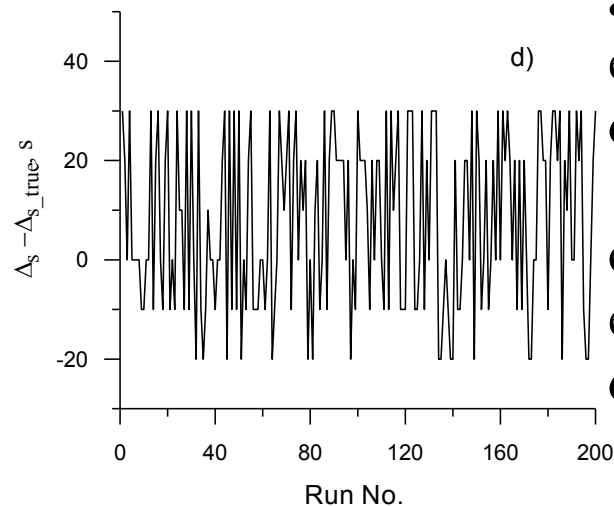
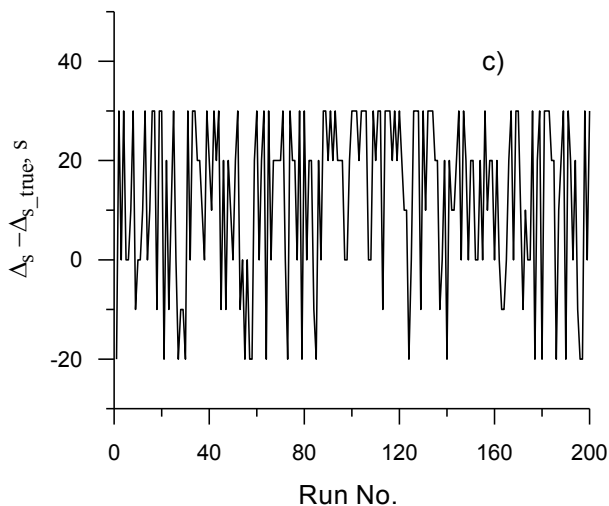
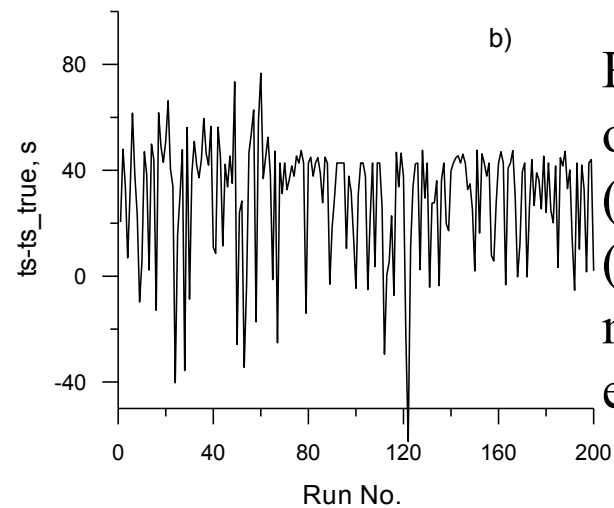
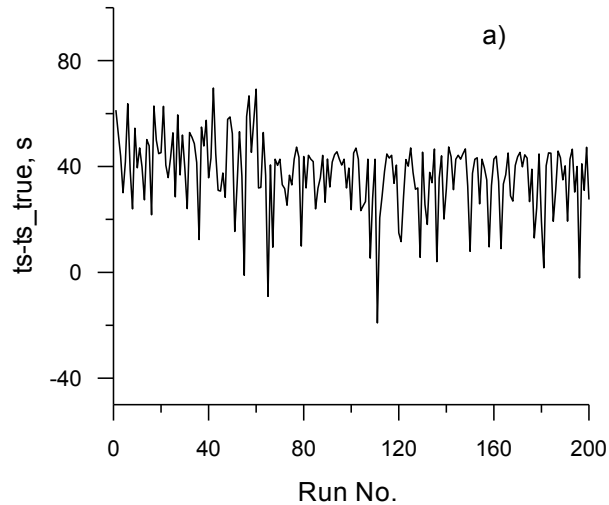


Results of source inversion obtained on the coarse grid (a,c,e) and on the fine grid (b,d,f) for different ensemble members of CUTE-3 experiment. The following results are shown:

- horizontal distance from estimated to true source (a,b);
- vertical coordinate of estimated source (c,d);
- difference between estimated and true release inventories (e,f).

Two points in circles shown on the bottom figure denote large values of estimated differences in released inventories which fall outside the plot boundaries and equal to 1443 and 574 kg respectively.

Results of calculations using observations from individual puffs (II)

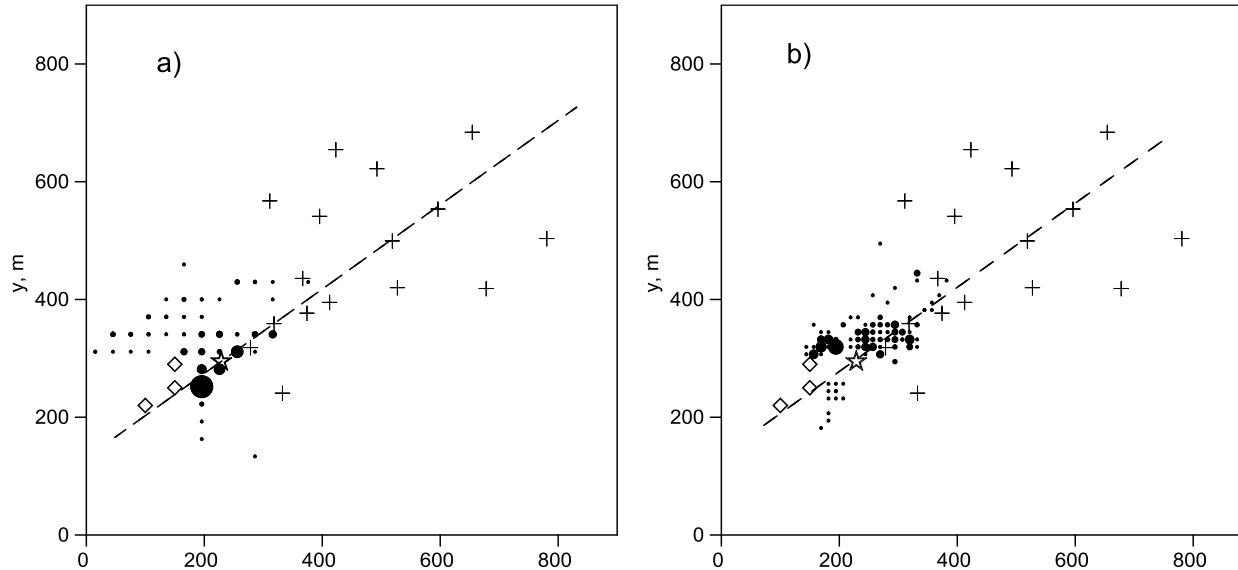


Results of source inversion obtained on the coarse grid (a,c) and on the fine grid (b,d) for different ensemble members of CUTE-3 experiment:

a),b) - difference between estimated and true start time of the release $t^s - t_t^s$

c),d) - differences between estimated and true release durations $\Delta^s - \Delta_t^s$

Results of calculations using observations from individual puffs (III)



Spatial distribution^{x, m} of the estimated xy coordinates of the source with using measurement values from different runs of the CUTE-3 experiments;

- a) – results obtained on the coarse grid;
- b) – results on fine grid;

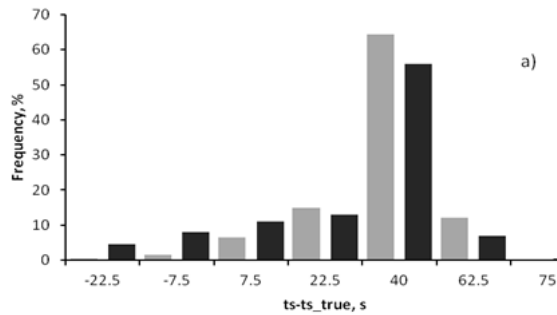
circles (●) denote estimated source location; the size of circle is proportional to a number m of cases when solution converged to corresponding location; the maximum size of circle correspond to $m=36$ (a) and $m=9$ (b);

meaning of the symbols ‘+’, ‘◇’ – the same as before. Dashed line is oriented along wind direction.

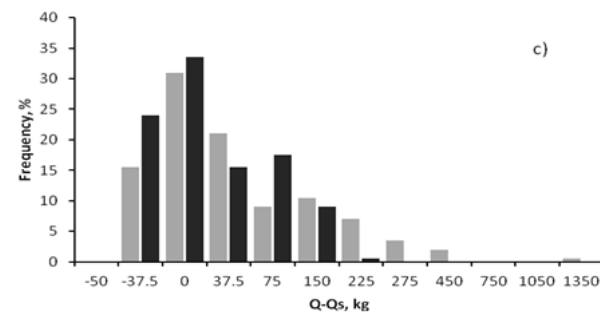
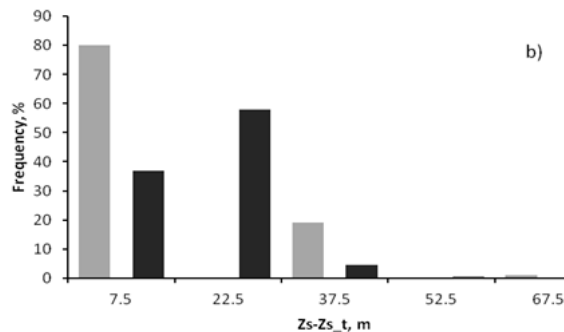
Results of calculations using observations from individual puffs (IV)

| PARAMETER | MEDIAN | MEAN | STDEV | SKEW | RMSE |
|---|--------|--------|--------|-------|--------|
| Coarse grid | | | | | |
| Dist, m | 54.50 | 74.68 | 51.54 | 1.20 | 90.63 |
| Dist_{along}, m | -34.60 | -16.27 | 62.55 | 0.35 | 64.48 |
| Dist_{cross}, m | -8.23 | -29.22 | 56.73 | -0.64 | 63.69 |
| $z^s - z_{true}^s$, m | 13.50 | 19.17 | 11.67 | 1.81 | 22.43 |
| $q^s - q_{true}^s$, kg | 27.98 | 64.74 | 138.85 | 5.49 | 152.89 |
| $t^s - t_{true}^s$, s | 40.28 | 37.00 | 14.13 | -0.86 | 39.59 |
| $\Delta^s - \Delta_{true}^s$, s | 20.00 | 12.45 | 16.79 | -0.58 | 20.87 |
| Fine grid | | | | | |
| Dist, m | 64.73 | 70.72 | 33.62 | 1.70 | 78.49 |
| Dist_{along}, m | 36.12 | 33.11 | 59.43 | 0.21 | 67.90 |
| Dist_{cross}, m | -23.22 | -23.05 | 32.02 | 0.03 | 39.39 |
| $z^s - z_{true}^s$, m | 18.00 | 17.04 | 10.58 | 0.73 | 20.04 |
| $q^s - q_{true}^s$, kg | 17.57 | 23.14 | 52.57 | 0.74 | 57.31 |
| $t^s - t_{true}^s$, s | 37.78 | 29.65 | 22.58 | -1.20 | 37.24 |
| $\Delta^s - \Delta_{true}^s$, s | 0.00 | 7.75 | 17.20 | -0.05 | 18.83 |

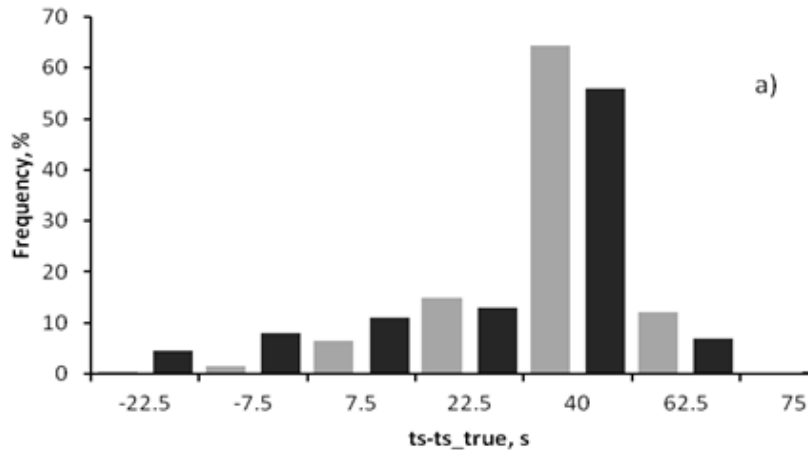
Results of calculations using observations from individual puffs (V)



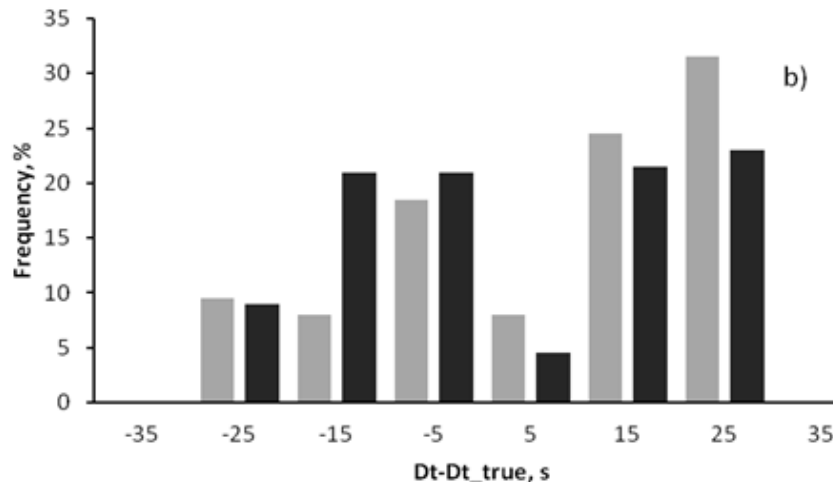
Frequency distributions of horizontal (a) and vertical (b) distances from the estimated to true source location, and difference between estimated and true released inventories (c) obtained in source inversion runs on coarse (grey color) and fine (black color) grids.



Results of calculations using observations from individual puffs (VI)



Frequency distributions of differences between estimated and true start time of the release $t^s - t_t^s$ (a) and difference between estimated and true release duration $\Delta^s - \Delta_t^s$ (n).



Conclusions

- CFD-based source inversion method suitable for real-time application.
- Applicable to cases of transient atmospheric dispersion in urban environment.
- Allows for identification of source location, inventory, start time, duration.
- Restricted to case of stationary meteorology and short duration release.

Future work

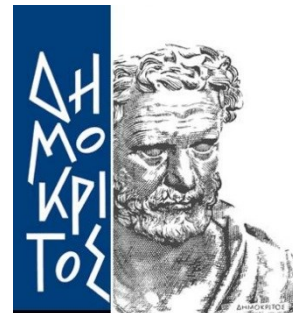
The algorithm has a great potential for parallelization because in direct minimization algorithm presented above the cost function could be calculated for each of the grid nodes independently of the others.

More information about the work

- 1) Kovalets et al., 2017. Inverse identification of unknown finite-duration air pollutant releases in urban environment, submitted in Environmental Modelling & Software.
- 2) ResearchGate, doi: [10.13140/RG.2.2.27474.45760/1](https://doi.org/10.13140/RG.2.2.27474.45760/1)
- 3) Email us:
Dr Ivan Kovalets: ik@env.com.ua
Dr George Efthimiou: gefthimiou@ipta.demokritos.gr

Acknowledgments

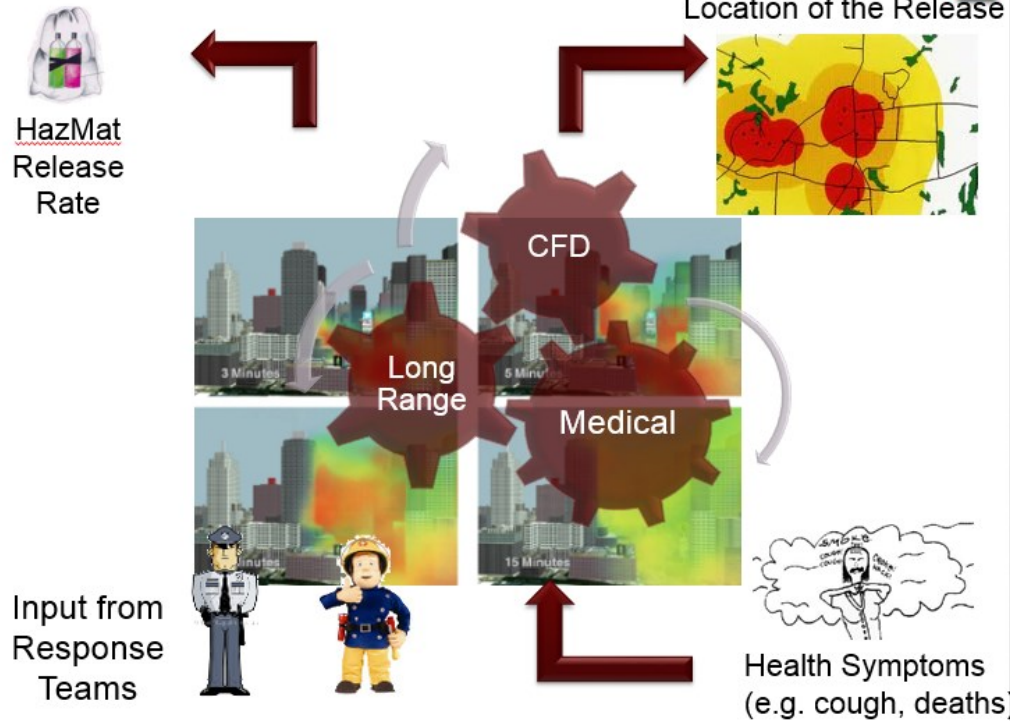
This publication was made possible by a NPRP award [NPRP 7-674-2-252] from the Qatar National Research Fund (a member of The Qatar Foundation). The statements made herein are solely the responsibility of the authors.



New achievement

Source reconstruction from Health Symptoms

6



Professor Kakosimos:
k.kakosimos@qatar.tamu.edu

Message from Dr Ivan Kovalets (I)

I published on LinkedIn a post regarding assessments of ruthenium sources with the aid of the JRODOS:

<https://www.linkedin.com/pulse/potential-sources-ruthenium-ivan-kovalets/>

May be you find it useful.

Best regards,

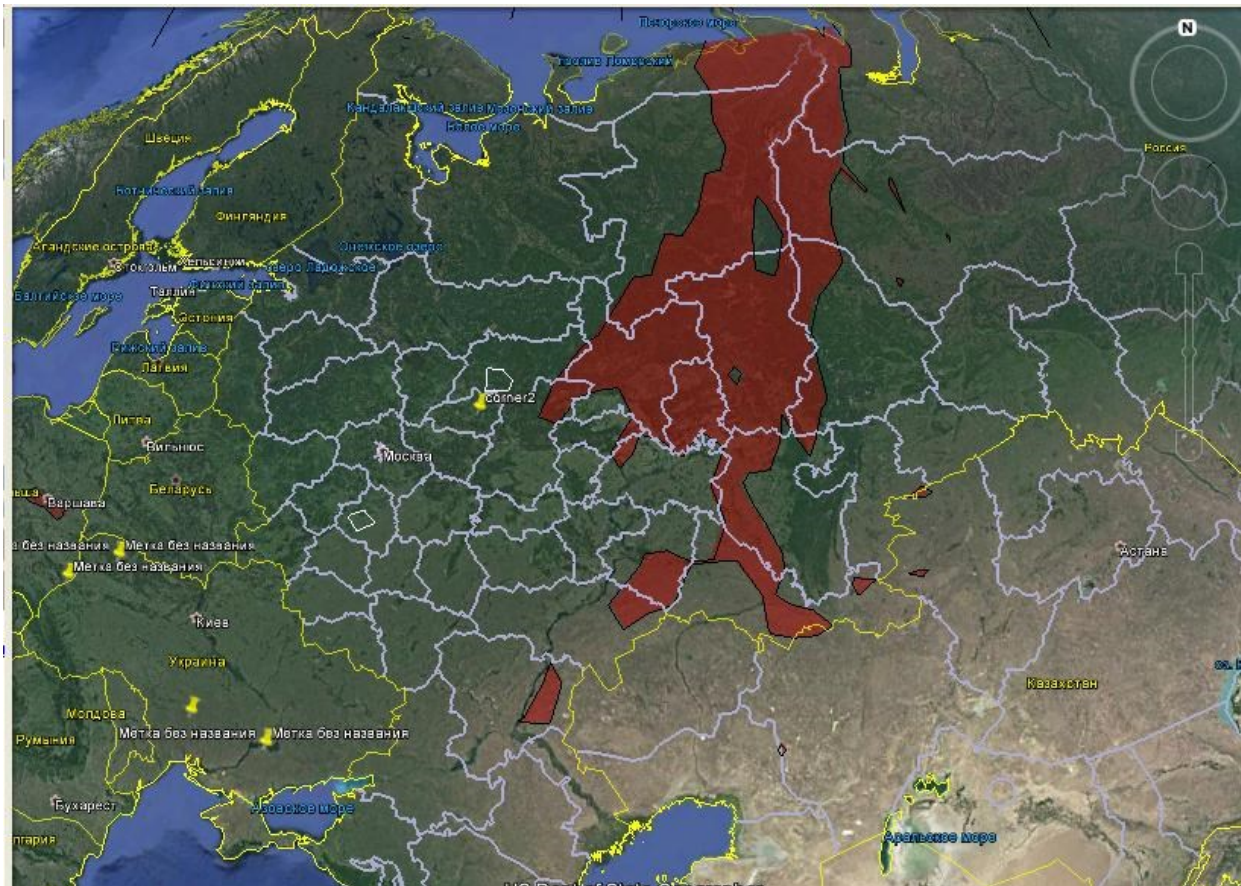
Ivan

Message from Dr Ivan Kovalets (II)

- I applied method to establish source of ruthenium-106 (you probably know that these days concentrations of ruthenium are increased over Europe).
- The results are consistent with what IRSN writes (http://www.irsn.fr/EN/newsroom/News/Pages/20171009_Detection-of-ruthenium-106-in-the-air-in-the-east-and-southeast-of-Europe.aspx)).

Message from Dr Ivan Kovalets (III)

- Figure presents preliminary estimates of the territory (in red) from which emissions could happen. The assessment did not use a map of nuclear installations, so the territory can be narrowed. Release located within 'red' territory, lasting 6 hours, and happening somewhere within the period from 24.09 to 02.10 leads to the correlation coefficient of the model as compared to measurements $>90\%$.



Message from Dr Ivan Kovalets (IV)

- Measurements were taken from the territory of Ukraine, Poland (to 06.10), Sweden, Switzerland (to 02.10), France, Czech Republic (to 04.10). At the next iteration, I will use the new data (also from CTBTO stations in Russia) and see how will they affect the assessment of the territories.
- The calculations (in inverse mode) were carried out with the JRODOS-MATCH. How we solve backward adjoint equation with RODOS MATCH is described here [https://www.researchgate.net/publication/317359018 SOLUTION OF THE SOURCE IDENTIFICATION PROBLEM WITH USING THE JRODOS MATCH](https://www.researchgate.net/publication/317359018_SOLUTION_OF_THE_SOURCE_IDENTIFICATION_PROBLEM_WITH_USING_THE_JRODOS_MATCH)
- The rest of the method is as described in EMS and HARMO18 papers.

Message from Dr Ivan Kovalets (V)

- Though the scale of the problem is completely different and hence in contrast to cited paper:
 - 1) we didn't use assumption of stationary meteorological fields and all the related modifications;
 - 2) we didn't estimate start time of the release and time bounds within which it belongs from the 'meteorological' considerations, but rather used expert evaluations.

Thank you for your attention